

# $\Lambda_c^+$ - and $\Lambda_b$ -hypernuclei

K. Tsushima<sup>1 \*</sup>, F.C. Khanna<sup>2 †</sup>

<sup>1</sup>Department of Physics and Astronomy, University of Georgia, Athens, GA 30602, USA

<sup>2</sup>CSSM, University of Adelaide, Adelaide, SA 5005, Australia

May 21, 2019

## Abstract

$\Lambda_c^+$ - and  $\Lambda_b$ -hypernuclei are studied in the quark-meson coupling (QMC) model. Comparisons are made with the results for  $\Lambda$ -hypernuclei studied in the same model previously. Although the scalar and vector potentials felt by the  $\Lambda$ ,  $\Lambda_c^+$  and  $\Lambda_b$  in the corresponding hypernuclei multiplet which has the same baryon numbers are quite similar, the wave functions obtained, e.g., for  $1s_{1/2}$  state, are very different. The  $\Lambda_c^+$  baryon density distribution in  $^{209}_{\Lambda_c^+}\text{Pb}$  is much more pushed away from the center than that for the  $\Lambda$  in  $^{209}_{\Lambda}\text{Pb}$  due to the Coulomb force. On the contrary, the  $\Lambda_b$  baryon density distributions in  $\Lambda_b$ -hypernuclei are much larger near the origin than those for the  $\Lambda$  in the corresponding  $\Lambda$ -hypernuclei due to its heavy mass. It is also found that level spacing for the  $\Lambda_b$  single-particle energies is much smaller than that for the  $\Lambda$  and  $\Lambda_c^+$ .

*PACS number(s)*: 24.85, 14.20.L, 14.20.M, 21.80, 21.65

*Keywords*:  $\Lambda_c^+$ - and  $\Lambda_b$ -hypernuclei, Single-particle energy levels, Density distributions, Quark-meson coupling model

---

\*tsushima@physast.uga.edu

†Permanent address: Department of Physics, University of Alberta, Edmonton, Canada, T6G 2J1  
khanna@Phys.UAlberta.CA

Recently we have made a systematic study of the changes in properties of the heavy hadrons which contain a charm or a bottom quark in nuclear matter [1]. The results suggest that the formations of charmed and bottom hypernuclei, which were predicted first in mid 70's [2, 3], are quite likely. The experimental possibilities were also studied later [4]. In addition, we predicted the  $B^-$ -nuclear (atomic) bound states, based on analogy with kaonic atom [5], and a study was made for the  $D$ - and  $\bar{D}$ -nuclear bound states [6] using the quark-meson coupling (QMC) model [7, 8, 9, 10]. The QMC model, which was used there and is used in this study, has been successfully applied to many problems associated with nuclear physics and hadronic properties in nuclear medium [11].

In this article, we make a quantitative study for the  $\Lambda_c^+$ - and  $\Lambda_b$ -hypernuclei, by solving a system of equations for finite nuclei embedding a  $\Lambda_c^+$  or a  $\Lambda_b$  in nucleus. Then, the results are compared with those for the  $\Lambda$ -hypernuclei [10], which were studied in QMC. It is shown that, although the scalar and vector potentials felt by the  $\Lambda$ ,  $\Lambda_c^+$  and  $\Lambda_b$  in the corresponding hypernuclei multiplet which has the same baryon numbers are quite similar, the wave functions obtained, e.g., for  $1s_{1/2}$  state are very different. Namely, the  $\Lambda_c^+$  baryon density distribution in  $^{209}_{\Lambda_c^+}\text{Pb}$  is much more pushed away from the center than that for the  $\Lambda$  in  $^{209}_{\Lambda}\text{Pb}$  due to the Coulomb force. On the contrary, the  $\Lambda_b$  baryon density distributions in  $\Lambda_b$ -hypernuclei are much more central than those for the  $\Lambda$  in the corresponding  $\Lambda$ -hypernuclei due to its heavy mass. In addition it turns out that the level spacing for the  $\Lambda_b$  single-particle energies is much smaller than that for the  $\Lambda$  and  $\Lambda_c^+$ , which may imply many interesting new phenomena, which will be discovered in due course by experiments. We hope this study opens a new possibility for experiments, related to nuclear and hadronic physics, especially for Japan Hadron Facility (JHF).

Using the Born-Oppenheimer approximation, a relativistic Lagrangian density which gives the same mean-field equations of motion for a charmed or a bottom hypernucleus, in which the quasi-particles moving in single-particle orbits are three-quark clusters with the quantum numbers of a charmed baryon, a bottom baryon or a nucleon, when expanded to the same order in velocity, is given by QMC [8, 9, 10]:

$$\begin{aligned}
\mathcal{L}_{QMC}^{CHY} &= \mathcal{L}_{QMC} + \mathcal{L}_{QMC}^C, \\
\mathcal{L}_{QMC} &= \bar{\psi}_N(\vec{r}) \left[ i\gamma \cdot \partial - M_N^*(\sigma) - (g_\omega \omega(\vec{r}) + g_\rho \frac{\tau_3^N}{2} b(\vec{r}) + \frac{e}{2}(1 + \tau_3^N) A(\vec{r})) \gamma_0 \right] \psi_N(\vec{r}) \\
&\quad - \frac{1}{2}[(\nabla \sigma(\vec{r}))^2 + m_\sigma^2 \sigma(\vec{r})^2] + \frac{1}{2}[(\nabla \omega(\vec{r}))^2 + m_\omega^2 \omega(\vec{r})^2] \\
&\quad + \frac{1}{2}[(\nabla b(\vec{r}))^2 + m_\rho^2 b(\vec{r})^2] + \frac{1}{2}(\nabla A(\vec{r}))^2, \\
\mathcal{L}_{QMC}^C &= \sum_{C=\Lambda_c^+, \Lambda_b} \bar{\psi}_C(\vec{r}) \left[ i\gamma \cdot \partial - M_C^*(\sigma) - (g_\omega^C \omega(\vec{r}) + g_\rho^C I_3^C b(\vec{r}) + eQ_C A(\vec{r})) \gamma_0 \right] \psi_C(\vec{r}), \quad (1)
\end{aligned}$$

where  $\psi_N(\vec{r})$  ( $\psi_C(\vec{r})$ ) and  $b(\vec{r})$  are respectively the nucleon (charmed and bottom baryon) and the  $\rho$  meson (the time component in the third direction of isospin) fields, while  $m_\sigma$ ,  $m_\omega$  and  $m_\rho$  are the masses of the  $\sigma$ ,  $\omega$  and  $\rho$  meson fields.  $g_\omega$  and  $g_\rho$  are the  $\omega$ - $N$  and  $\rho$ - $N$  coupling constants which are related to the corresponding  $(u, d)$ -quark- $\omega$ ,  $g_\omega^q$ , and  $(u, d)$ -quark- $\rho$ ,  $g_\rho^q$ , coupling constants as  $g_\omega = 3g_\omega^q$  and  $g_\rho = g_\rho^q$  [8, 9]. Hereafter we will use notations for the quark flavors,  $q \equiv u, d$  and  $Q \equiv s, c, b$ .

In an approximation where the  $\sigma$ ,  $\omega$  and  $\rho$  fields couple only to the  $u$  and  $d$  quarks, the coupling constants in the charmed and bottom baryons are obtained as  $g_\omega^C = (n_q/3)g_\omega$ , and  $g_\rho^C \equiv g_\rho = g_\rho^q$ , with  $n_q$  being the total number of valence  $u$  and  $d$  (light) quarks in the baryon  $C$ .  $I_3^C$  and  $Q_C$  are the third component of the baryon isospin operator and its electric charge in units of the proton charge,  $e$ , respectively. The field dependent  $\sigma$ - $N$  and  $\sigma$ - $C$  coupling strengths predicted by the QMC model,  $g_\sigma(\sigma)$  and  $g_\sigma^C(\sigma)$ , related to the Lagrangian density, Eq. (1), at the hadronic level are defined by:

$$M_N^*(\sigma) \equiv M_N - g_\sigma(\sigma)\sigma(\vec{r}), \quad (2)$$

$$M_C^*(\sigma) \equiv M_C - g_\sigma^C(\sigma)\sigma(\vec{r}), \quad (3)$$

where  $M_N$  ( $M_C$ ) is the free nucleon (charmed and bottom baryon) mass (masses). Note that the dependence of these coupling strengths on the applied scalar field must be calculated self-consistently within the quark model [8, 9, 10]. Hence, unlike quantum hadrodynamics (QHD) [12], even though  $g_\sigma^C(\sigma)/g_\sigma(\sigma)$  may be 2/3 or 1/3 depending on the number of light quarks in the baryon in free space ( $\sigma = 0$ )<sup>1</sup>, this will not necessarily be the case in nuclear matter. More explicit expressions for  $g_\sigma^C(\sigma)$  and  $g_\sigma(\sigma)$  will be given later. From the Lagrangian density, Eq. (1), a set of equations of motion for the charm or bottom hypernuclear system is obtained,

$$[i\gamma \cdot \partial - M_N^*(\sigma) - (g_\omega\omega(\vec{r}) + g_\rho\frac{\tau_3^N}{2}b(\vec{r}) + \frac{e}{2}(1 + \tau_3^N)A(\vec{r}))\gamma_0]\psi_N(\vec{r}) = 0, \quad (4)$$

$$[i\gamma \cdot \partial - M_C^*(\sigma) - (g_\omega^C\omega(\vec{r}) + g_\rho I_3^C b(\vec{r}) + eQ_C A(\vec{r}))\gamma_0]\psi_C(\vec{r}) = 0, \quad (5)$$

$$\begin{aligned} (-\nabla_r^2 + m_\sigma^2)\sigma(\vec{r}) &= -[\frac{\partial M_N^*(\sigma)}{\partial\sigma}]\rho_s(\vec{r}) - [\frac{\partial M_C^*(\sigma)}{\partial\sigma}]\rho_s^C(\vec{r}), \\ &\equiv g_\sigma C_N(\sigma)\rho_s(\vec{r}) + g_\sigma^C C_C(\sigma)\rho_s^C(\vec{r}), \end{aligned} \quad (6)$$

$$(-\nabla_r^2 + m_\omega^2)\omega(\vec{r}) = g_\omega\rho_B(\vec{r}) + g_\omega^C\rho_B^C(\vec{r}), \quad (7)$$

$$(-\nabla_r^2 + m_\rho^2)b(\vec{r}) = \frac{g_\rho}{2}\rho_3(\vec{r}) + g_\rho^C I_3^C \rho_B^C(\vec{r}), \quad (8)$$

$$(-\nabla_r^2)A(\vec{r}) = e\rho_p(\vec{r}) + eQ_C\rho_B^C(\vec{r}), \quad (9)$$

where,  $\rho_s(\vec{r})$  ( $\rho_s^C(\vec{r})$ ),  $\rho_B(\vec{r})$  ( $\rho_B^C(\vec{r})$ ),  $\rho_3(\vec{r})$  and  $\rho_p(\vec{r})$  are the scalar, baryon, third component of isovector, and proton densities at the position  $\vec{r}$  in the charmed or bottom hypernuclei [8, 9, 10]. On the right hand side of Eq. (6),  $-[\frac{\partial M_N^*(\sigma)}{\partial\sigma}] = g_\sigma C_N(\sigma)$  and  $-[\frac{\partial M_C^*(\sigma)}{\partial\sigma}] = g_\sigma^C C_C(\sigma)$ , where  $g_\sigma \equiv g_\sigma(\sigma = 0)$  and  $g_\sigma^C \equiv g_\sigma^C(\sigma = 0)$ , are a new, and characteristic feature of QMC beyond QHD [12, 13, 14]. The effective mass for the charmed or bottom baryon  $C$  is defined by,

$$\frac{\partial M_C^*(\sigma)}{\partial\sigma} = -n_q g_\sigma^q \int_{bag} d\vec{y} \bar{\psi}_q(\vec{y})\psi_q(\vec{y}) \equiv -n_q g_\sigma^q S_C(\sigma) = -\frac{\partial}{\partial\sigma} [g_\sigma^C(\sigma)\sigma], \quad (10)$$

with the MIT bag model quantities [7, 8, 9, 10],

$$M_C^*(\sigma) = \sum_{j=q,Q} \frac{n_j \Omega_j^* - z_C}{R_C^*} + \frac{4}{3}\pi(R_C^*)^3 B,$$

---

<sup>1</sup>Strictly, this is true only when the bag radii of nucleon and baryon  $C$  are exactly the same in the present model. See the last line in Eq. (11).

$$\begin{aligned}
S_C(\sigma) &= \frac{\Omega_q^*/2 + m_q^* R_C^* (\Omega_q^* - 1)}{\Omega_q^* (\Omega_q^* - 1) + m_q^* R_C^* / 2}, \\
\Omega_q^* &= \sqrt{x_q^2 + (R_C^* m_q^*)^2}, \quad \Omega_Q^* = \sqrt{x_Q^2 + (R_C^* m_Q^*)^2}, \quad m_q^* = m_q - g_\sigma^q \sigma(\vec{r}), \\
C_C(\sigma) &= S_C(\sigma)/S_C(0), \quad g_\sigma^C \equiv n_q g_\sigma^q S_C(0) = \frac{n_q}{3} g_\sigma S_C(0)/S_N(0) \equiv \frac{n_q}{3} g_\sigma \Gamma_{C/N}. \quad (11)
\end{aligned}$$

Quantities for the nucleon are similarly obtained by replacing the indices,  $C \rightarrow N$ . Here,  $z_C$ ,  $B$ ,  $x_{q,Q}$ , and  $m_{q,Q}$  are the parameters for the sum of the c.m. and gluon fluctuation effects, bag pressure, lowest eigenvalues for the quarks,  $q$  or  $Q$ , respectively, and the corresponding current quark masses.  $z_N$  and  $B$  ( $z_C$ ) are fixed by fitting the nucleon (charmed or bottom baryon) mass in free space.

The bag radii in-medium,  $R_{N,C}^*$ , are obtained by the equilibrium condition  $dM_{N,C}^*(\sigma)/dR_{N,C}|_{R_{N,C}=R_{N,C}^*} = 0$ . The bag parameters calculated and chosen for the present study in free space are,  $(z_N, z_\Lambda, z_{\Lambda_c^+}, z_{\Lambda_b}) = (3.295, 3.131, 1.766, -0.643)$ ,  $(R_N, R_\Lambda, R_{\Lambda_c^+}, R_{\Lambda_b}) = (0.800, 0.806, 0.846, 0.930)$  fm,  $B^{1/4} = 170$  MeV,  $(m_q, m_s, m_c, m_b) = (5, 250, 1300, 4200)$  MeV. The parameters associated with the  $u$ ,  $d$  and  $s$  quarks are the same as in our previous investigations [9, 10]. At the hadron level, the entire information on the quark dynamics is condensed in  $C_{N,C}(\sigma)$  of Eq. (6). The parameters at the hadron level, which are already fixed by the study of infinite nuclear matter and finite nuclei [9], are as follows:  $m_\omega = 783$  MeV,  $m_\rho = 770$  MeV,  $m_\sigma = 418$  MeV,  $e^2/4\pi = 1/137.036$ ,  $g_\omega^2/4\pi = 3.12$ ,  $g_\rho^2/4\pi = 5.31$  and  $g_\sigma^2/4\pi = 6.93$ .

We briefly discuss about the spin-orbit force in QMC [8]. The origin of the spin orbit force for a composite nucleon moving through scalar and vector fields which vary with position was explained in detail in Ref. [8] – c.f. sect. 3.2. The situation for the  $\Lambda$  and also for other hyperons are discussed in detail in Ref. [10].

In order to include the spin-orbit potential (approximately) correctly, e.g., for the  $\Lambda_c^+$ , we add perturbatively the correction due to the vector potential,  $-\frac{2}{2M_{\Lambda_c^+}^*} \left( \frac{d}{dr} g_\omega^\Lambda \omega(\vec{r}) \right) \vec{l} \cdot \vec{s}$ , to the single-particle energies obtained with the Dirac equation, in the same way as that added in Ref. [10]. This may correspond to a correct spin-orbit force which is calculated by the underlying quark model [8, 10]:

$$V_{S.O.}^{\Lambda_c^+}(\vec{r}) \vec{l} \cdot \vec{s} = -\frac{1}{2M_{\Lambda_c^+}^* \vec{r}} \left( \frac{d}{dr} [M_{\Lambda_c^+}^*(\vec{r}) + g_\omega^{\Lambda_c^+} \omega(\vec{r})] \right) \vec{l} \cdot \vec{s}, \quad (12)$$

since the Dirac equation at the hadronic level solved in usual QHD-type models leads to:

$$V_{S.O.}^{\Lambda_c^+}(\vec{r}) \vec{l} \cdot \vec{s} = -\frac{1}{2M_{\Lambda_c^+}^* \vec{r}} \left( \frac{d}{dr} [M_{\Lambda_c^+}^*(\vec{r}) - g_\omega^{\Lambda_c^+} \omega(\vec{r})] \right) \vec{l} \cdot \vec{s}, \quad (13)$$

which has the opposite sign for the vector potential,  $g_\omega^{\Lambda_c^+} \omega(\vec{r})$ . The correction to the spin-orbit force, which appears naturally in the QMC model, may also be modelled at the hadronic level of the Dirac equation by adding a tensor interaction.

However, in practice, because of its heavy mass ( $M_{\Lambda_c^+}^*$ ), contribution to the single-particle energies from the spin-orbit potential with or without including the correction term, turned out to be even smaller than that for the  $\Lambda$ -hypernuclei, and further smaller for the  $\Lambda_b$ -hypernuclei. Contribution from the spin-orbit potential with the correction term is typically of order 0.01

MeV, and even for the largest case is  $\cong 0.1$  MeV. This can be understood when one considers the limit,  $M_{\Lambda_c^+}^* \rightarrow \infty$  in Eq. (12), where the quantity inside the square brackets varies smoothly from an order of hundred MeV to zero near the surface of the hypernucleus, and the derivative with respect to  $r$  is finite. (See also Figs. 2 and 3.)

Now we discuss the results. First, we show in Fig. 1 the total baryon density distributions in  ${}^{41}_j\text{Ca}$  and  ${}^{209}_j\text{Pb}$  ( $j = \Lambda, \Lambda_c^+, \Lambda_b$ ), for  $1s_{1/2}$  configuration in each hypernucleus. Note that because of the self-consistency, the total baryon density distributions are dependent on the configurations of the embedded particles. The total baryon density distributions are quite similar for the  $\Lambda$ -,  $\Lambda_c^+$ - and  $\Lambda_b$ -hypernuclei multiplet which has the same baryon numbers,  $A$ , since the effect of  $\Lambda, \Lambda_c^+$  and  $\Lambda_b$  is  $\cong 1/A$  for each hypernucleus. Nevertheless, one notices that the  $\Lambda_b$ -hypernuclei density near the center is slightly higher than the corresponding  $\Lambda$ - and  $\Lambda_c^+$ -hypernuclei. This is because the  $\Lambda_b$  is heavy and localized nearer the center, and contributes to the total baryon density there. The baryon (probability) density distributions for the  $\Lambda, \Lambda_c^+$  and  $\Lambda_b$  in corresponding hypernuclei will be shown later.

Next, in Figs. 2 and 3, we show the scalar and vector potentials felt by the  $\Lambda, \Lambda_c^+$  and  $\Lambda_b$  for  $1s_{1/2}$  state, in  ${}^{41}_j\text{Ca}$  and  ${}^{209}_j\text{Pb}$  ( $j = \Lambda, \Lambda_c^+, \Lambda_b$ ). For the  $\Lambda_c^+$ , the Coulomb potentials are also shown. As for the case of the nuclear matter [1], the scalar and vector potentials felt by these particles in hypernuclei multiplet which has the same baryon numbers are also quite similar. Thus, as far as the total baryon density distributions and the scalar and vector potentials are concerned,  $\Lambda$ -,  $\Lambda_c^+$ - and  $\Lambda_b$ -hypernuclei show quite similar features within the multiplet. Of course, the Coulomb force for the  $\Lambda_c^+$  plays a crucial role in giving much smaller binding for realistic nuclei.

Having obtained reasonable ideas about the potentials felt by  $\Lambda, \Lambda_c^+$  and  $\Lambda_b$ , we show the calculated single-particle energies in Tables 1 and 2. Results for the  $\Lambda$ -hypernuclei are from Ref. [10]. In these calculations, effective Pauli blocking, and correction to the spin-orbit force based on the underlying quark structure, are included as discussed earlier [10]. (However, recall that the negligibly small contribution from the correction terms for the spin-orbit force, and also contributions from the spin-orbit force itself.) In addition, we searched for the single-particle states up to the same highest state as that of the core neutrons in each hypernucleus, since the deeper levels are usually easier to observe in experiment.

In Tables 1 and 2, it is clear that the  $\Lambda_c^+$  single-particle energy levels are higher than the corresponding levels for the  $\Lambda$  and  $\Lambda_b$ . This is a consequence of the Coulomb force. This feature becomes stronger as the proton number in the core nucleus increases.

Second, the level spacing for the  $\Lambda_b$  single-particle energies is much smaller than that for the  $\Lambda$  and  $\Lambda_c^+$ . This may be ascribed to its heavy mass (or  $M_b^*$ ). In the Dirac equation for the  $\Lambda_b$ , the mass term dominates more than that of the term proportional to Dirac's  $\kappa$ , which classifies the states, or single-particle wave functions. (See Refs. [9, 10] for detail.) This small level spacing would make it very difficult to distinguish the states in experiment, or to achieve such high resolution. On the other hand, this may imply also many new phenomena. It will have a large probability to trap a  $\Lambda_b$  among one of those many states, especially in heavy nucleus such as Pb. What are the consequences? May be the  $\Lambda_b$  weak decay happens inside a heavy nucleus with a very low probability? Does it emit many photons when the  $\Lambda_b$  gradually makes transitions from a deeper state to a shallower state? All these questions raise a flood of speculations.

To summarize, we have made a quantitative study for  $\Lambda_c^+$ - and  $\Lambda_b$ -hypernuclei in a quark-

meson coupling model. We have solved a system of equations in a self-consistent approach for several finite nuclei with closed shell plus a hyperon ( $\Lambda_c^+$  or  $\Lambda_b$ ), embedding a  $\Lambda_c^+$  or  $\Lambda_b$  in the nucleus. Results are compared with those for the  $\Lambda$ -hypernuclei. It is shown that, although the scalar and vector potentials felt by the  $\Lambda$ ,  $\Lambda_c^+$  and  $\Lambda_b$  are quite similar in corresponding hypernuclei multiplet which has the same baryon numbers, the single-particle wave functions, and single-particle energy level spacings are quite different. For the  $\Lambda_c^+$ -hypernuclei, the Coulomb force plays a crucial role, and so does the heavy  $\Lambda_b$  mass for the  $\Lambda_b$ -hypernuclei. It should be emphasized that we have used the values for the coupling constants of  $\sigma$  (or  $\sigma$ -field dependent strength),  $\omega$  and  $\rho$  to the  $\Lambda$ ,  $\Lambda_c^+$  and  $\Lambda_b$  determined automatically based on the underlying quark model, as for the nucleon and other baryons. (Recall that the values for the vector  $\omega$  fields to any baryons can be obtained by the number of light quarks in a baryon, but those for the  $\sigma$  are different as shown in Eqs. (10) and (11).) Phenomenology would determine ultimately if the coupling constants (strengths) determined by the underlying quark model actually work for  $\Lambda_c^+$  and  $\Lambda_b$  or not. Although implications of the present results can be speculated a great deal, we would like to emphasize that, what we showed is that the  $\Lambda_c^+$ - and  $\Lambda_b$ -hypernuclei would exist in realistic experimental conditions. Experiments at facilities like JHF would provide further inputs to gain a better understanding of the interaction of  $\Lambda_c^+$  and  $\Lambda_b$  with the nuclear matter. Additional studies are needed to investigate the semi-leptonic weak decay of  $\Lambda_c^+$  and  $\Lambda_b$  hyperons. The role of Pauli blocking and density in influencing the decay rates as compared to the free hyperons would be highly useful. Such study can have an impact on the hadronization of the quark-gluon plasma and the transport of hadrons in nuclear matter of high density. Will the high density lead to a slower decay and that a higher probability to survive its passage through the material ? At present the study of the presence of  $\Lambda_c^+$  and  $\Lambda_b$  in finite nuclei is its infancy. Careful investigations, both theoretical and experimental, would lead to a much better understanding of the role of heavy quarks in finite nuclei.

#### Acknowledgment

The authors would like to thank Prof. A.W. Thomas for the hospitality at the CSSM, Adelaide, where this work was initiated. K.T. acknowledges support and warm hospitality at University of Alberta, where this work was completed. K.T. is supported by the Forschungszentrum-Jülich, contract No. 41445282 (COSY-058). The work of F.K. is supported by NSERCC.

## References

- [1] K. Tsushima, F.C. Khanna, nucl-th/0207036.
- [2] A.A. Tyapkin, Sov. J. Nucl. Phys. 22 (1976) 89.
- [3] C.B. Dover and S.H. Kahana, Phys. Rev. Lett. 39 (1977) 1506.
- [4] T. Bressani, F. Iazzi, Nuovo. Cim. 102 A (1989) 597;  
S.A. Buyatov, V.V. Lyukov, N.I. Strakov and V.A. Tsarev, Nuovo. Cim. 104 A (1991) 1361.

- [5] T.M. Ito, R.S. Hayano, S.N. Nakamura, and T.P. Terada, Phys. Rev. C 58 (1998) 2366; M. Iwasaki, Nucl. Phys. A 670 (2000) 190c; S. Hirenzaki, Y. Okumura, H. Toki, E. Oset, and A. Ramos, Phys. Rev. C 61 (2000) 055205.
- [6] K. Tsushima, D.H. Lu, A.W. Thomas, K. Saito, R.H. Landau, Phys. Rev. C 59 (1999) 2824.
- [7] P.A.M. Guichon, Phys. Lett. B 200 (1989) 235.
- [8] P.A.M. Guichon, K. Saito, E.N. Rodionov, A.W. Thomas Nucl. Phys. A 601 (1996) 349.
- [9] K. Saito, K. Tsushima, A.W. Thomas, Nucl. Phys. A 609 (1996) 339.
- [10] K. Tsushima, K. Saito, A.W. Thomas, Phys. Lett. B 411 (1997) 9; (E) *ibid.* B 421 (1998) 413; K. Tsushima, K. Saito, J. Haidenbauer, A.W. Thomas, Nucl. Phys. A 630 (1998) 691.
- [11] K. Saito, K. Tsushima, A.W. Thomas, Phys. Rev. C 55 (1997) 2637; Phys. Rev. C 56 (1997) 566; G. Krein, A.W. Thomas, K. Tsushima, Nucl. Phys. A 650 (1999) 313; K. Tsushima, K. Saito, A.W. Thomas, S.V. Wright, Phys. Lett. B 429 (1998) 239; (E) *ibid.* B 436 (1998) 453; K. Tsushima, A. Sibirtsev, A.W. Thomas, Phys. Rev. C 62 (2000) 064904; J. Phys. G 27 (2001) 349; K. Tsushima D.H. Lu, A.W. Thomas, K. Saito, Phys. Lett. B 443 (1998) 26; D.H. Lu, K. Tsushima, A.W. Thomas, A.G. Williams, K. Saito, Nucl. Phys. A 634 (1998) 443; K. Tsushima, in the proceeding, *ISHEP 98*, Dubna, Russia, 17-22 Aug 1998, nucl-th/9811063; Nucl. Phys. A 670 (2000) 198c; K. Tsushima, A. Sibirtsev, K. Saito, A.W. Thomas, D.H. Lu, Nucl. Phys. A 680 (2001) 280c; W. Melnitchouk, K. Tsushima, A.W. Thomas, Eur. Phys. J. A14 (2002) 105; K. Tsushima, hep-ph/0206069.
- [12] J.D. Walecka, Ann. Phys. (N.Y.) 83 (1974) 491; B.D. Serot and J.D. Walecka, Adv. Nucl. Phys. 16 (1986) 1.
- [13] M. Rufa, H. Stöcker, P-G Reinhard, J. Maruhn and W. Greiner, J. Phys. G13 (1987) L143.
- [14] E.D. Cooper, B.K. Jennings, J. Mareš, Nucl. Phys. A 580 (1994) 419; J. Mareš and B.K. Jennings, Phys. Rev. C 49 (1994) 2472; J. Mareš, B.K. Jennings and E.D. Cooper, Prog. Theor. Phys. Supp. 117 (1994) 415; J. Mareš and B.K. Jennings, Nucl. Phys. A 585 (1995) 347c; J. Mareš, E. Friedman, A. Gal, B.K. Jennings, Nucl. Phys. A 594 (1995) 311.
- [15] R.E. Chrien **A478** (1988) 705c.
- [16] S. Ajimura et al., Nucl. Phys. **A585** (1995) 173c.

Table 1: Single-particle energies (in MeV) for  ${}^{17}_j\text{O}$ ,  ${}^{41}_j\text{Ca}$  and  ${}^{49}_j\text{Ca}$  ( $j = \Lambda, \Lambda_c^+, \Lambda_b$ ). Single-particle energy levels are calculated up to the same highest states as that of the core neutrons. Results for the hypernuclei are taken from Ref. [10]. Experimental data for  $\Lambda$ -hypernuclei are taken from Ref. [15], where spin-orbit splittings for  $\Lambda$ -hypernuclei are not well determined by the experiments.

	${}^{16}_{\Lambda}\text{O}$ (Exp.)	${}^{17}_{\Lambda}\text{O}$	${}^{17}_{\Lambda_c^+}\text{O}$	${}^{17}_{\Lambda_b}\text{O}$	${}^{40}_{\Lambda}\text{Ca}$ (Exp.)	${}^{41}_{\Lambda}\text{Ca}$	${}^{41}_{\Lambda_c^+}\text{Ca}$	${}^{41}_{\Lambda_b}\text{Ca}$	${}^{49}_{\Lambda}\text{Ca}$	${}^{49}_{\Lambda_c^+}\text{Ca}$	${}^{49}_{\Lambda_b}\text{Ca}$
$1s_{1/2}$	-12.5	-14.1	-12.8	-19.6	-20.0	-19.5	-12.8	-23.0	-21.0	-14.3	-24.4
$1p_{3/2}$	-2.5	-5.1	-7.3	-16.5	-12.0	-12.3	-9.2	-20.9	-13.9	-10.6	-22.2
$1p_{1/2}$	( $1p_{3/2}$ )	-5.0	-7.3	-16.5	( $1p_{3/2}$ )	-12.3	-9.1	-20.9	-13.8	-10.6	-22.2
$1d_{5/2}$						-4.7	-4.8	-18.4	-6.5	-6.5	-19.5
$2s_{1/2}$						-3.5	-3.4	-17.4	-5.4	-5.3	-18.8
$1d_{3/2}$						-4.6	-4.8	-18.4	-6.4	-6.4	-19.5
$1f_{7/2}$									—	-2.0	-16.8



Table 2: Single-particle energies (in MeV) for  $^{91}_j\text{Zr}$  and  $^{208}_j\text{Pb}$  ( $j = \Lambda, \Lambda_c^+, \Lambda_b$ ). Experimental data are taken from Ref. [16]. See caption of Table 1 for other explanations.

	$^{89}_{\Lambda}\text{Yb}$ (Exp.)	$^{91}_{\Lambda}\text{Zr}$	$^{91}_{\Lambda_c^+}\text{Zr}$	$^{91}_{\Lambda_b}\text{Zr}$	$^{208}_{\Lambda}\text{Pb}$ (Exp.)	$^{209}_{\Lambda}\text{Pb}$	$^{209}_{\Lambda_c^+}\text{Pb}$	$^{209}_{\Lambda_b}\text{Pb}$
$1s_{1/2}$	-22.5	-23.9	-10.8	-25.7	-27.0	-27.0	-5.2	-27.4
$1p_{3/2}$	-16.0	-18.4	-8.7	-24.2	-22.0	-23.4	-4.1	-26.6
$1p_{1/2}$	( $1p_{3/2}$ )	-18.4	-8.7	-24.2	( $1p_{3/2}$ )	-23.4	-4.0	-26.6
$1d_{5/2}$	-9.0	-12.3	-5.8	-22.4	-17.0	-19.1	-2.4	-25.4
$2s_{1/2}$	—	-10.8	-3.9	-21.6	—	-17.6	—	-24.7
$1d_{3/2}$	( $1d_{5/2}$ )	-12.3	-5.8	-22.4	( $1d_{5/2}$ )	-19.1	-2.4	-25.4
$1f_{7/2}$	-2.0	-5.9	-2.4	-20.4	-12.0	-14.4	—	-24.1
$2p_{3/2}$	—	-4.2	—	-19.5	—	-12.4	—	-23.2
$1f_{5/2}$	( $1f_{7/2}$ )	-5.8	-2.4	-20.4	( $1f_{7/2}$ )	-14.3	—	-24.1
$2p_{1/2}$		-4.1	—	-19.5	—	-12.4	—	-23.2
$1g_{9/2}$		—	—	-18.1	-7.0	-9.3	—	-22.6
$1g_{7/2}$					( $1g_{9/2}$ )	-9.2	—	-22.6
$1h_{11/2}$						-3.9	—	-21.0
$2d_{5/2}$						-7.0	—	-21.7
$2d_{3/2}$						-7.0	—	-21.7
$1h_{9/2}$						-3.8	—	-21.0
$3s_{1/2}$						-6.1	—	-21.3
$2f_{7/2}$						-1.7	—	-20.1
$3p_{3/2}$						-1.0	—	-19.6
$2f_{5/2}$						-1.7	—	-20.1
$3p_{1/2}$						-1.0	—	-19.6
$1i_{13/2}$						—	—	-19.3

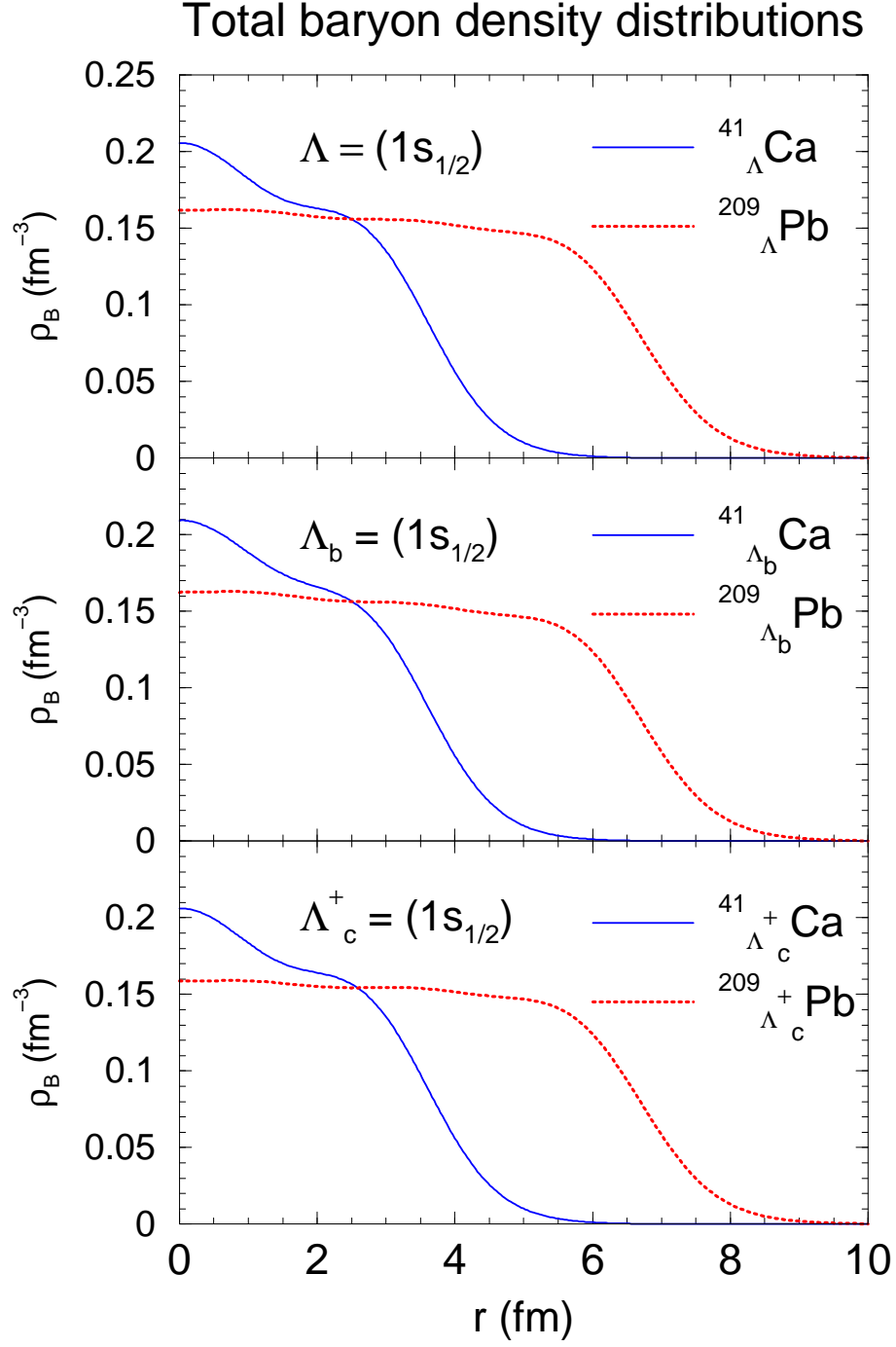


Figure 1: Total baryon density distributions in  $^{41}_j \text{Ca}$  and  $^{209}_j \text{Pb}$  ( $j = \Lambda, \Lambda_c^+, \Lambda_b$ ), for  $1s_{1/2}$  configuration for the  $\Lambda, \Lambda_c^+$  and  $\Lambda_b$ .

## Scalar and vector potentials in $^{41}\text{Ca}$

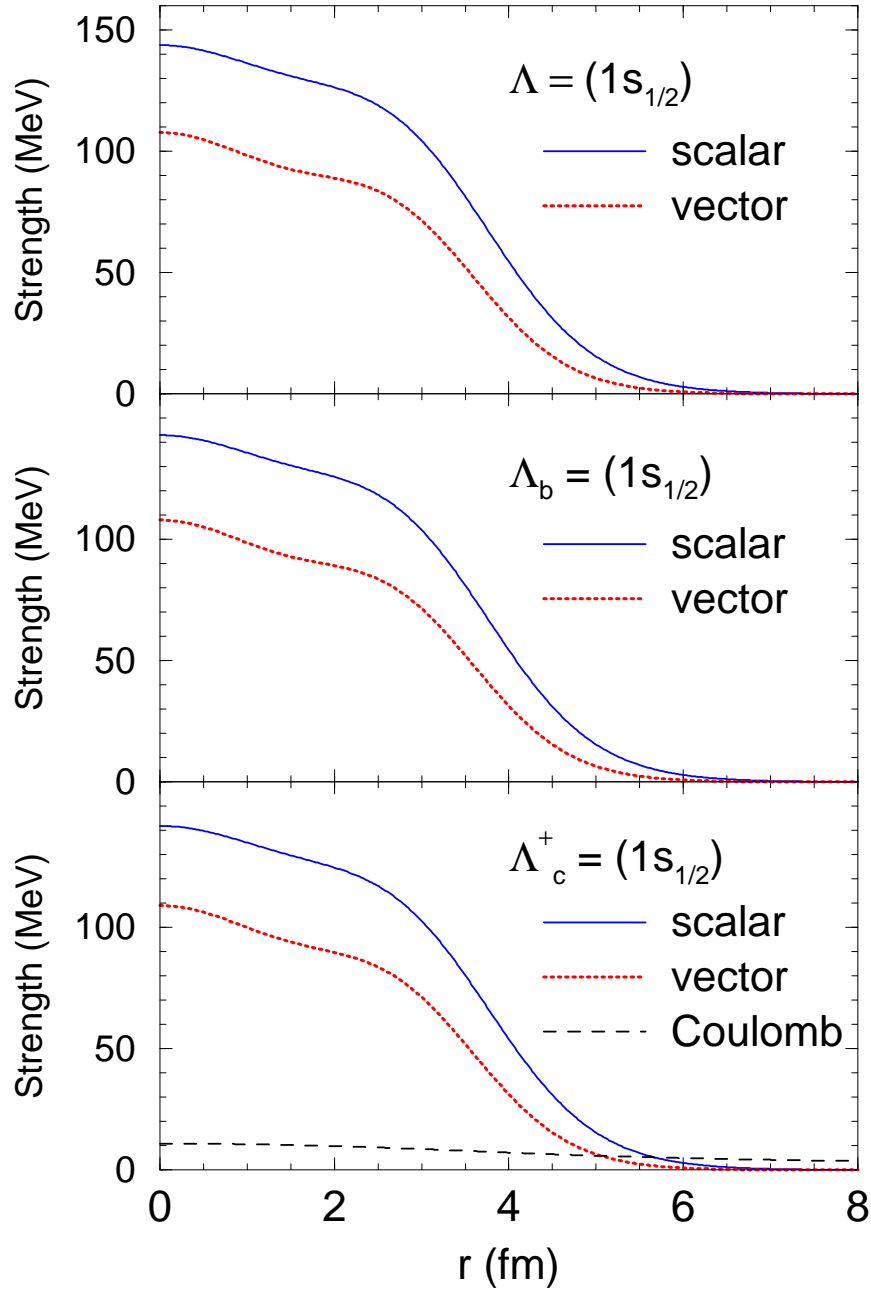


Figure 2: Potential strengths for  $1s_{1/2}$  state felt by the  $\Lambda$ ,  $\Lambda_c^+$  and  $\Lambda_b$  in  $^{41}\text{Ca}$  ( $j = \Lambda, \Lambda_c^+, \Lambda_b$ ).

# Scalar and vector potentials in $^{209}\text{Pb}$

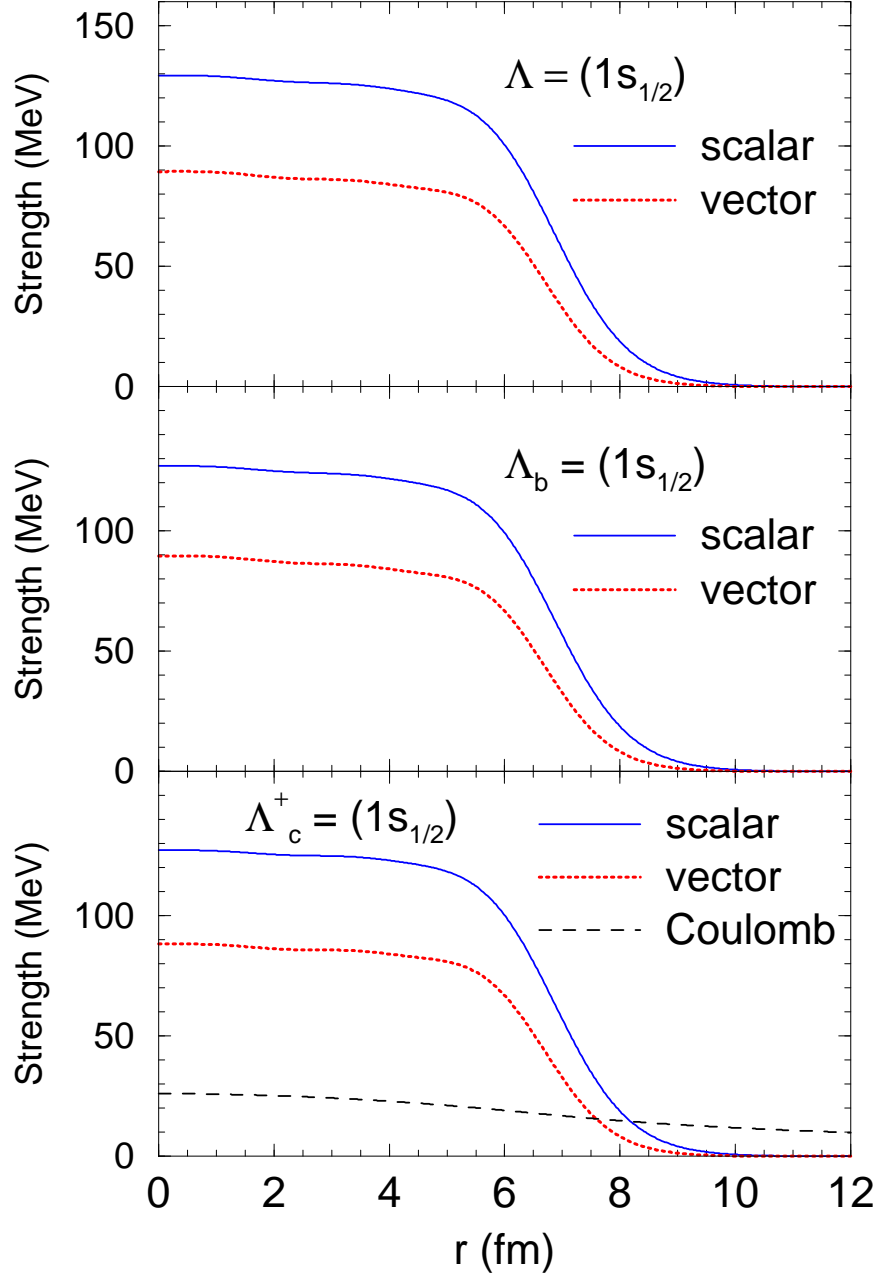


Figure 3: Potential strengths for  $1s_{1/2}$  state felt by the  $\Lambda$ ,  $\Lambda_c^+$  and  $\Lambda_b$  in  $^{209}_j\text{Pb}$  ( $j = \Lambda, \Lambda_c^+, \Lambda_b$ ).

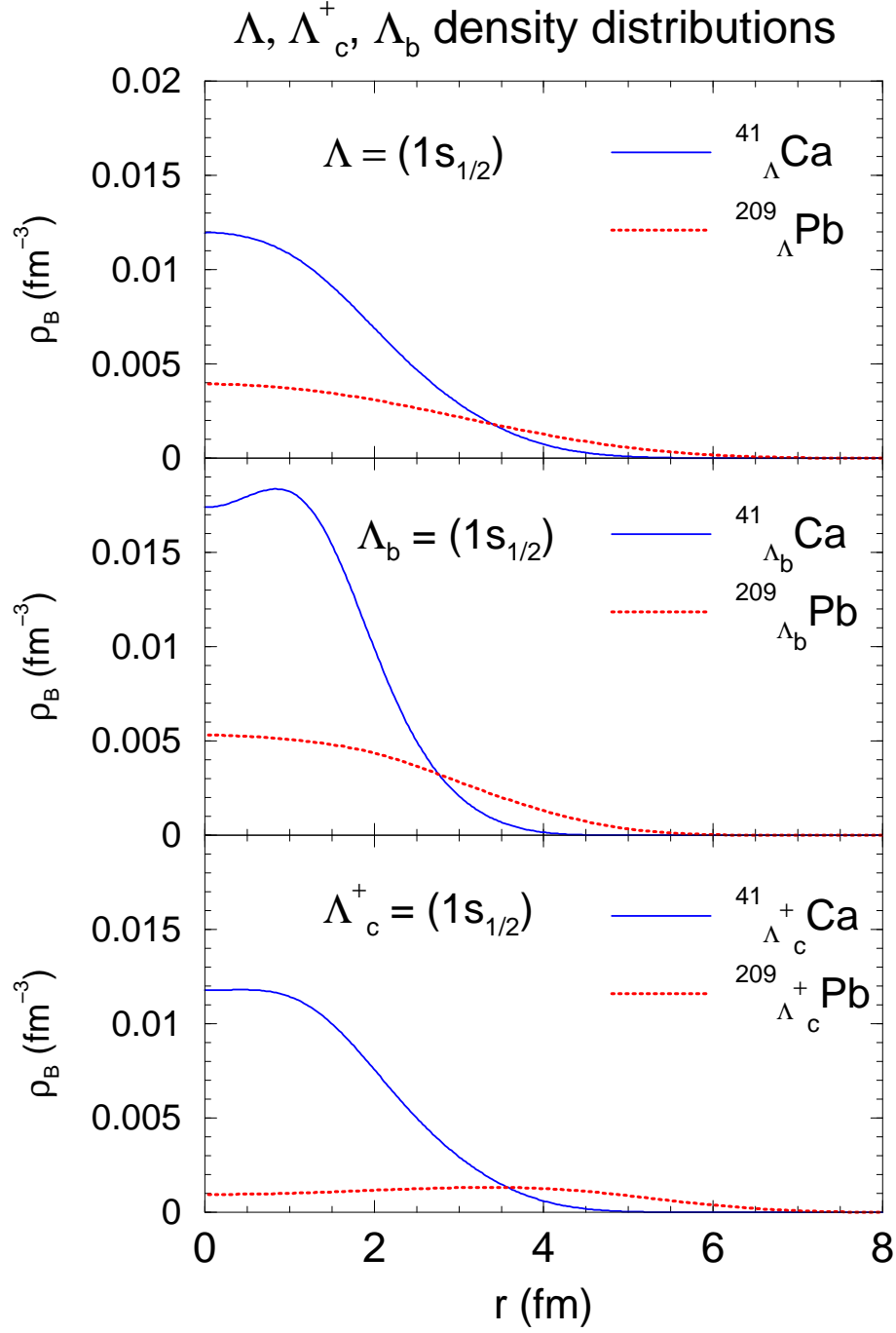


Figure 4:  $\Lambda, \Lambda_c^+$  and  $\Lambda_b$  baryon (probability) density distributions for  $1s_{1/2}$  state in  $^{41}_j\text{Ca}$  and  $^{209}_j\text{Pb}$  ( $j = \Lambda, \Lambda_c^+, \Lambda_b$ ).